DOI: 10.1002/cbic.200800343

Amyloid Fibrillar Meshwork Formation of Iron-Induced Oligomeric Species of Aβ40 with Phthalocyanine Tetrasulfonate and Its Toxic Consequences

Jae-Woo Park,[a] Jung Sun Ahn,[a] Jung-Ho Lee,[a] Ghibom Bhak,[a] Seunho Jung,[b] and Seung R. Paik*[a]

Amyloid-β protein (Aβ) is a pathological component of Alzheimer's disease (AD) that participates in the senile plaque formation in the neocortex of the patient's brain.[1] Aβ is generated from the ubiquitous amyloid precursor protein (APP) through proteolysis by β and γ-secretases.[2,3] Abnormal accumulation of Aβ is believed to cause the neuronal degeneration that is selective to the cholinergic neurons in particular.[4] Self-association of Aβ leads to various fibrillation states, such as soluble high-molecular-weight oligomeric forms, globular species, which are known as Aβ-derived diffusible ligands, protofibrils as metastable intermediates, and finally amyloid fibrils.[5,6] Although the toxic species has not been defined unequivocally, the prefibrillar assemblies of Aβ are considered to be responsible for the neuronal degeneration by affecting the stability of biological membranes.[7] Besides this Aβ-only hypothesis of exert neurotoxicity, metals have been also suggested to act as an additional toxic component within the Aβ amyloids.[8–11] Those metals, including iron, copper, and zinc would provide a pivotal center for reactive oxygen species (ROS) generation at the expense of endogenous reducing agents.[12,13] For treatment strategies of AD, therefore, suppression of Aβ production, clearance of the toxic prefibillar species with anti-Aβ antibodies, antioxidants, and metal-chelating agent have been extensively tested.[14–18] Because the neurodegeneration that is observed in AD is induced from multifactorial causes, a novel therapeutic strategy that concomitantly handles some of the multiple causal candidates at the same time is highly recommendable.

We herein introduce phthalocyanine tetrasulfonate (PcTS) as a cyclic tetrapyrrole compound with a planar and hydrophobic central aromatic macrocyclic structure, which accommodates various metal ions. Metal-containing PcTS tends to self-assemble into nanoparticles, monolayers, and thin films.[19–22] By taking advantage of those properties of metal chelation and molecular self-assembly, PcTS has been employed not only to remove the redox-active metals from the toxic metal-induced oligomeric species of Aβ40 but also to convert the protofibrillar species into an amyloid fibrillar meshwork if possible (Scheme 1). This dual function of PcTS, therefore, could take care of the toxic consequences of the prefibrillar species due to the membrane destabilization by the oligomeric structures

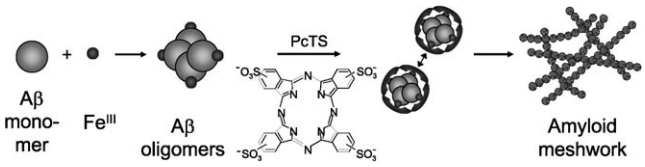

Scheme 1. PcTS treatment of the metal-induced oligomeric species of Aβ40.

as well as the oxidative stress by the redox-active metal ions. PcTS was previously demonstrated to be an anti-scrapie compound that interfered with the pathological conversion of prion protein to the protease-resistant form.[23] The compound was also shown to suppress the amyloid fibril formation of α-synuclein, which is responsible for the pathogenesis of Parkinson's disease (PD).[24]

Metal-induced oligomeric granular structures of Aβ40 were obtained by treating 60 μM Aβ40 with 40 μM $FeCl_3$ in 20 mM Tris–HCl, pH 7.0, that contained 0.1 M NaCl, for 3 h at 37 °C (Figure 1A).

Those oligomeric structures could also be derived with 1 μM $FeCl_3$ for 12 μM Aβ40 during a relatively short (0.5 to 1 h) incubation at 37 °C. The average diameter of the oligomers was estimated to be 20 nm, with a height of 1.6 nm from the AFM image. Upon PcTS treatment at 50 μM for additional 27 h under a quiescent incubation condition, an extensive meshwork of Aβ40 amyloid fibrils was surprisingly produced even though a suppression of the metal-induced fibrillation was also equally probable (Figure 1B). Those oligomeric Aβ40 species that were obtained with 1 μM Fe^{III} also turned into the discrete amyloid fibrils following the PcTS treatment (data not shown). The β-sheet content of the fibrillar meshwork was confirmed with CD spectroscopy. Although the Fe^{III}-induced oligomeric species of Aβ40 still contained mainly a random structure with a minor shift of the minimum ellipticity from 195 nm to 202 nm, the PcTS-treated species exhibited a drastic structural change to a β-sheet conformation with a minimum ellipticity at 218 nm (Figure 1C). The dramatic granule-to-fibril conversion, however, was not observed when Aβ40 was incubated under the same conditions (27 h at 37 °C) in the absence (Figure 1E) or separate presence of PcTS (Figure 1F), $FeCl_3$ (Figure 1G), and PcTS–Fe^{III} complex (Figure 1H). Those Aβ40 fibrils (Figures 1E–H) showed rather heterogeneous distribution of protofibrillar to fibrillar structures, in which the longest fibrils were far shorter than the fibrils that were observed in the meshwork (Figure 1B). In addition, the presence of NaCl

[a] J.-W. Park, J. S. Ahn, J.-H. Lee, G. Bhak, Dr. S. R. Paik
School of Chemical and Biological Engineering
Seoul National University
Seoul 151–744 (Korea)
Fax: (+82) 2-888-1604
E-mail: srpaik@snu.ac.kr

[b] Dr. S. Jung
Department of Bioscience and Biotechnology, Konkuk University
Seoul 143–701 (Korea)

Supporting information for this article is available on the WWW under http://www.chembiochem.org or from the author: details of the experimental procedures for the hydroxyl radical production assay, the culture of SH-SY5Y cells, and the cytotoxicity assay employing trypan blue.

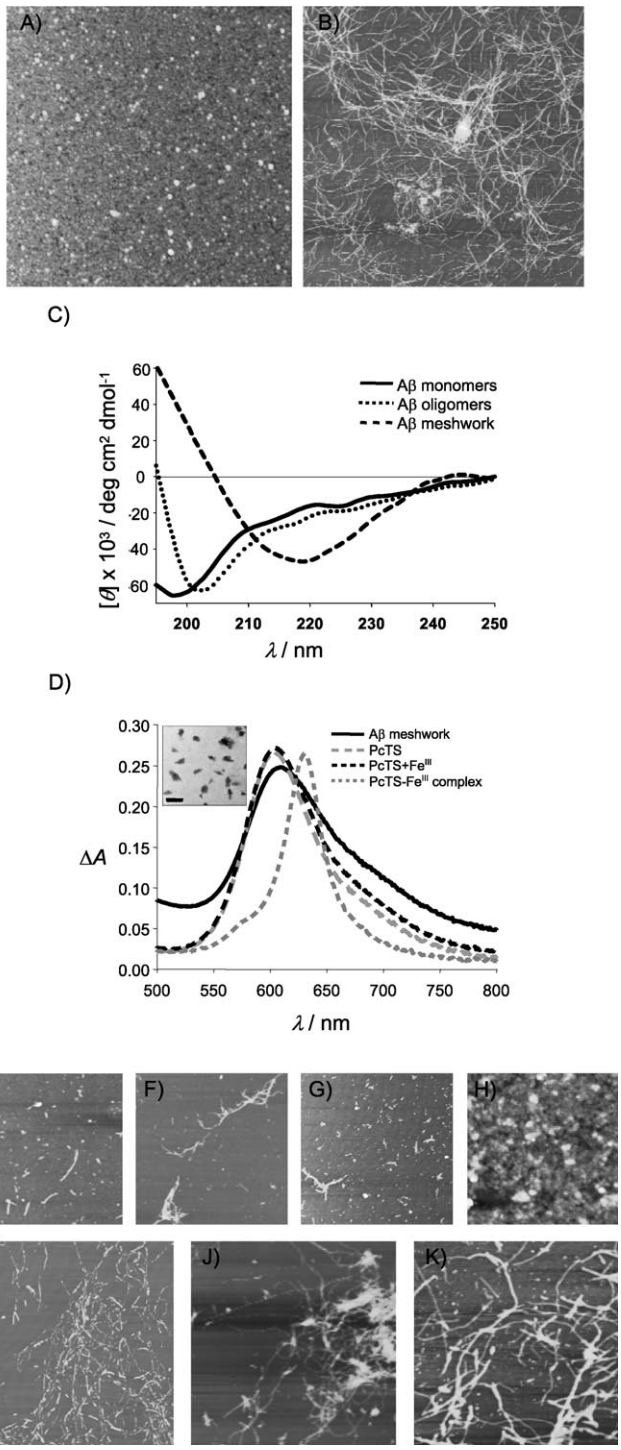

Figure 1. AFM images (5×5 μm) of A) Aβ40 oligomers prepared with Fe^{III}, B) PcTS-induced Aβ40 fibrillar meshwork derived from the iron-mediated oligomers. C) CD spectra of the Aβ40 species in monomeric, oligomeric, and meshwork states. D) Absorbance spectra of PcTS in the presence and absence of Fe^{III}, PcTS–Fe^{III} complex, and the PcTS-induced Aβ40 meshwork. Self-assembled structures of the PcTS–Fe^{III} complex obtained in the absence of Aβ40 (inset, the scale bar for 0.2 μm.). AFM images of the Aβ40 incubation products for 30 h with E) Aβ40 alone, F) Aβ40+PcTS, G) Aβ40+$FeCl_3$, H) Aβ40+PcTS–Fe^{III} complex. AFM images (5×5 μm) of PcTS-induced products of the metal-induced Aβ40 prefibrillar structures obtained with I) Cu^{II}, J) Zn^{II}, K) Al^{III}.

turned out to be critical for the meshwork formation, which might be required to neutralize the sulfonate groups in PcTS for the molecular self-assembly process.

To evaluate the iron interaction with PcTS during the meshwork formation, a set of absorbance experiments was also carried out (Figure 1D). The PcTS and PcTS–Fe^{III} complex exhibited two distinctive absorption maxima at 604 and 631 nm, respectively. When PcTS was incubated with Fe^{III} in the absence of Aβ40, the iron was not chelated into PcTS under our experimental condition; this was determined by the absorption maximum, which did not shift from 604 nm. On the other hand, the Aβ40 meshwork that was prepared in the presence of Fe^{III} and PcTS exhibited an absorption maximum slightly red-shifted to 609 nm from 604 nm. The absorbance at 631 nm, however, was increased slightly from that of the PcTS and Fe^{III} incubation mixture obtained in the absence of Aβ40. Taken together with the fact that the PcTS–Fe^{III} complex has been assembled into the distinctive structures unlike the amyloid meshwork (Figure 1D, inset), it is pertinent to consider that the exact PcTS–Fe^{III} complex has not been generated during the meshwork formation. Additional undefined light absorbing structures, therefore, appeared to be formed between PcTS and Fe^{III} in the presence of Aβ40. It still requires, however, more careful chemical analysis before we conclusively define the precise nature of the molecular assembly involving PcTS and Fe^{III} for the Aβ40 meshwork formation.

The PcTS-induced fibrillation of Aβ40 was also examined with other metals such as Cu^{II}, Zn^{II}, and Al^{III} as additional risk factors for AD. The PcTS treatment at 50 μM for the metal-induced prefibrillar species of Aβ40 that was obtained in the presence of 40 μM each of the metals for total 27 h also gave rise to the amplified formation of fibrillar structures although they appeared to be different from each other under AFM. In the presence of copper, rather short fibrillar fragments were shown to be lined up to form long strands (Figure 1I). The image appears that brittle long fibrils are broken into short fragments; this indicates that the Cu^{II}/PcTS-mediated assembly of Aβ40 prefibrillar species might not be as strong as was observed with the Fe^{III}-mediated fibrillar meshwork formation. In the case of zinc, although long thin fibrils were revealed, the products were rather heterogeneous because they contained small aggregates scattered around the amorphous precipitate (Figure 1J). Aluminum also produced a fibrillar mesh, but the individual fibrils were much thicker than the fibrils that were obtained with other metals (Figure 1K). Because the metal interaction of Aβ40 has been demonstrated to be highly selective,[25–27] the meshworks that were produced with PcTS in the presence of the metals such as Fe^{III}, Cu^{II}, Zn^{II}, and Al^{III} have been distinctive for their morphologies. In addition, the specific metal interaction of PcTS and its participation in the assembly process could also play a role on the different meshwork formation.

Because PcTS could eradicate the toxic species of metal-induced oligomeric species of Aβ40 by converting them into the extensive fibrillar meshwork, we have examined PcTS to define its function as a detoxifying agent. Hydroxyl radical ($OH^{\bullet}$) generation by the redox-active iron present on either the oligo-

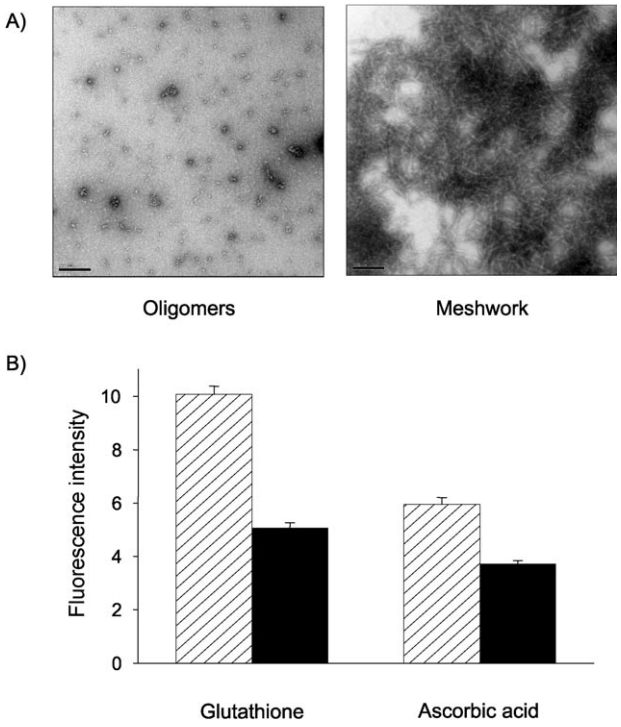

Figure 2. A) TEM images of Fe^{III}-induced Aβ40 oligomers and PcTS-induced amyloid meshwork obtained from the oligomers after 30 h of incubation. The scale bars represent 0.2 μm. B) Hydroxyl radical formation was assessed with TPA for the oligomers (striped bars) and the meshwork (black bars) in the presence of either glutathione or ascorbic acid.

mers or the meshwork was examined in the presence of H_2O_2 and either glutathione or ascorbic acid as a reducing agent. In the presence of 50 μM PcTS, the oligomeric structures obtained with 60 μM Aβ40 and 50 μM $FeCl_3$ after a 3 h incubation at 37 °C turned into the amyloid fibrillar meshwork after 27 h of incubation (Figure 2A). As the fibrillar meshwork became massive, the hydroxyl radical production by the metal ion decreased by 49.7% and 37.6% in the presence of glutathione and ascorbic acid, respectively (Figure 2B); this indicates that the reduction of Fe^{III} by the reducing agents was significantly prohibited within the PcTS-mediated amyloid meshwork. The metal chelation by PcTS, therefore, could control the redox-active property of iron that was bound to the amyloids in the presence of endogenous reducing species, which might suppress the ROS generation in general under pathological conditions.

Membrane destabilization by the metal-induced oligomeric structures of Aβ40 and their subsequent cytotoxic effects were directly evaluated with mammalian neuroblastoma SH-SY5Y cells. Because the cytotoxic effect of the particulate species was observed during the early phase of incubation in a locally restricted manner on the lawn of cells, individual cells were focused in terms of their morphological change and membrane permeabilization. The metal-induced oligomeric species transformed the cells into a round-shaped state, which led to cluster formation of the affected cells (Figure 3A); the formed meshwork appeared as a blue precipitate, but the cells remained intact (Figure 3C). Upon the trypan blue treatment,

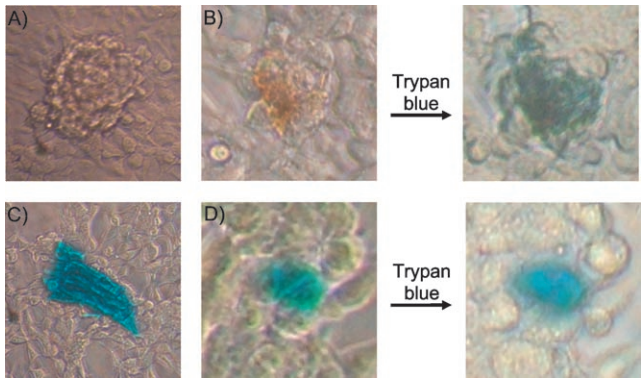

Figure 3. A) SH-SY5Y cells treated with the Fe^{III}-induced Aβ40 oligomers and B) their images with and without staining. C) SH-SY5Y cells treated with the PcTS-induced Aβ40 meshwork and D) their images before and after the trypan blue treatment.

the round-shaped cells became permeable to the dye (Figure 3B), but the meshwork-treated cells remained unaffected (Figure 3D). The fibrillar meshwork formation by PcTS treatment, therefore, is demonstrated to be adequate to deactivate the toxic oligomeric activity of intracellular invasion.

In this report, we have shown that PcTS exhibits its multitargeted detoxifying activity against the iron-induced oligomeric species of Aβ40 by transforming them into the amyloid fibrillar meshwork, which coincidentally eliminates both the redox-active metal ions and the toxic oligomeric structures at the same time—the two most likely toxic culprits for neurodegeneration in AD. The metal-chelating strategy has been widely recognized as an important approach to minimize the toxic consequences that are caused by the metal-mediated Aβ40 oligomers. Clioquinol (CQ) has been demonstrated to be an effective metal-chelating agent to detoxify the metal-mediated Aβ40 oligomers by converting them back to soluble Aβ40.[28] Coincidentally, CQ also inhibits the H_2O_2 production by metals such as Cu^{II} or Fe^{III} that are bound to the soluble (or insoluble) peptide.[29] Our PcTS, on the other hand, acts on the reverse direction by fixing the toxic metals of Aβ40 oligomers into the amyloid meshwork. Both metal-chelating agents, however, play a common function for removing the toxic metal-mediated Aβ40 oligomers. For a therapeutic application of PcTS, it needs to be further investigated whether the resulting meshwork itself could exhibit additional toxic effects on biological tissues because the meshwork formation would provide heterogeneous protein aggregates that could affect cellular biogenesis or cause damage to biological molecules by the photosensitive and redox-active metal–PcTS complexes.[30,31]

Experimental Section

Human Aβ40 was purchased from Sigma–Aldrich. The peptide concentration of Aβ40 in DMSO was spectrophotometrically determined to be 0.6 mM by monitoring absorbance at 276 nm with a molar extinction coefficient of 1450 $cm^{-1}\,M^{-1}$;[32] the stock solution was stored at −80 °C in aliquots. The peptide was diluted in Tris–HCl (20 mM, pH 7.5) that contained NaCl (0.1 M). Phthalocyanine

tetrasulfonate (PcTS) was from ICN Biomedical Inc. (Aurora, OH, USA). $FeCl_3$, $CuCl_2$, $ZnCl_2$, $AlCl_3$, hydrogen peroxide, terephthalic acid, glutathione, L-ascorbic acid, and trypan blue were obtained from Sigma–Aldrich. Carbon-coated copper grid (200 mesh) and uranyl acetate were from Ted Pella Inc. (Redding, CA, USA) and Electron Microscopy Sciences (Hatfield, PA, USA), respectively. A centrifugal membrane filter (YM-30) was purchased from Millipore. Dulbecco's Modified Eagle's Medium (DMEM) and fetal bovine serum were purchased from Hyclone (Logan, UT, USA). Trypsin–EDTA was provided by Gibco.

Aβ40 (60 μM) was preincubated with various metals (40 μM) in Tris–HCl (20 mM, pH 7.5) that contained NaCl (0.1 M), for 3 h at 37 °C. Phthalocyanine tetrasulfonate (PcTS, 50 μM) was added, and the solution was incubated for an additional 27 h at 37 °C.

Acknowledgements

This work was supported in part by Basic Research Program Grant from Korea Science and Engineering (R01-2007-000-20089-0) and a grant from the Seoul R&BD Program (10538).

Keywords: Alzheimer's disease · bioinorganic chemistry · phthalocyanines · protein structures · reactive oxygen species

[1] J. H. Morrison, P. R. Hof, *Science* **1997**, *278*, 412–419.
[2] P. E. Fraser, L. Lévesque, D. R. McLachlan, *Clin. Biochem.* **1993**, *26*, 339–349.
[3] F. Checler, *J. Neurochem.* **1995**, *65*, 1431–1444.
[4] P. Davies, A. J. F. Maloney, *Lancet* **1976**, *308*, 1403.
[5] M. Stefani, C. M. Dobson, *J. Mol. Med.* **2003**, *81*, 678–699.
[6] F. Chiti, C. M. Dobson, *Annu. Rev. Biochem.* **2006**, *75*, 333–366.
[7] N. Arispe, H. B. Pollard, E. Rojas, *Proc. Natl. Acad. Sci. USA* **1993**, *90*, 10573–10577.
[8] A. Campbell, M. A. Smith, L. M. Sayre, S. C. Bondy, G. Perry, *Brain Res. Bull.* **2001**, *55*, 125–132
[9] M. A. Deibel, W. D. Ehmann, W. R. Markesbery, *J. Neurol. Sci.* **1996**, *143*, 137–142.
[10] M. A. Lovell, J. D. Robertson, W. J. Teesdale, J. L. Campbell, W. R. Markesbery, *J. Neurol. Sci.* **1998**, *158*, 47–52.
[11] M. A. Smith, P. L. R. Harris, L. M. Sayre, G. Perry, *Proc. Natl. Acad. Sci. USA* **1997**, *94*, 9866–9868.
[12] X. Huang, C. S. Atwood, M. A. Hartshorn, G. Multhaup, L. E. Goldstein, R. C. Scarpa, M. P. Cuajungco, D. N. Gray, J. Lim, R. D. Moir, R. E. Tanzi, A. I. Bush, *Biochemistry* **1999**, *38*, 7609–7616.
[13] B. J. Tabner, S. Turnbull, O. M. A. El-Agnaf, D. Allsop, *Free Radical Biol. Med.* **2002**, *32*, 1076–1083.
[14] M. Citron, *Trends Pharmacol. Sci.* **2004**, *25*, 92–97.
[15] D. Schenk, *Nat. Rev. Neurosci.* **2002**, *3*, 824–828.
[16] C. A. Hawkes, J. McLaurin, *Expert Rev. Neurother.* **2007**, *7*, 1535–1548.
[17] C. Behl, *Prog. Neurobiol.* **1999**, *57*, 301–323.
[18] F. Molina-Holgado, R. C. Hider, A. Gaeta, R. Williams, P. Francis, *Biometals* **2007**, *20*, 639–654.
[19] X. Zhang, M. Gao, X. Kong, Y. Sun, J. Shen, *J. Chem. Soc. Chem. Commun.* **1994**, 1055–1056.
[20] Y. M. Lvov, G. N. Kamau, D. L. Zhou, J. F. Rusling, *J. Colloid Interface Sci.* **1999**, *212*, 570–575.
[21] Z. S. Chickneyan, A. L. Briseno, X. Shi, S. Han, J. Huang, F. Zhou, *J. Nanosci. Nanotechnol.* **2004**, *4*, 628–634.
[22] Y. Guan, S. H. Yu, M. Antonietti, C. Bottcher, C. F. J. Faul, *Chem. Eur. J.* **2005**, *11*, 1305–1311.
[23] S. A. Priola, A. Raines, W. S. Caughey, *Science* **2000**, *287*, 1503–1506.
[24] E. N. Lee, H. J. Cho, C. H. Lee, D. Lee, K. C. Chung, S. R. Paik, *Biochemistry* **2004**, *43*, 3704–3715.
[25] A. I. Bush, W. H. Pettingell, G. Multhaup, M. Paradis, J.-P. Vonsattel, J. F. Gusella, K. Beyreuther, C. L. Masters, R. E. Tanzi, *Science* **1994**, *265*, 1464–1467.
[26] A. I. Bush, R. D. Moir, K. M. Rosenkranz, R. E. Tanzi, *Science* **1995**, *268*, 1921–1923.
[27] C. S. Atwood, R. C. Scarpa, X. Huang, R. D. Moir, W. D. Jones, D. P. Fairlie, R. E. Tanzi, A. I. Bush, *J. Neurochem.* **2000**, *75*, 1219–1233.
[28] A. I. Bush, *Neurobiol. Aging* **2002**, *23*, 1031–1038.
[29] A. I. Bush, *Trends Neurosci.* **2003**, *26*, 207–214.
[30] Y. Çimen, H. Türk, *J. Mol. Catal. A: Chem.* **2007**, *265*, 237–243.
[31] Y. Çimen, H. Türk, *Appl. Catal. A* **2008**, *340*, 52–58.
[32] M. R. Nichols, M. A. Moss, D. K. Reed, W.-L. Lin, R. Mukhopadhyay, J. H. Hoh, T. L. Rosenberry, *Biochemistry* **2002**, *41*, 6115–6127.

Received: May 23, 2008
Published online on September 18, 2008

